Am J Physiol Lung Cell Mol Physiol 316: L1094–L1106, 2019.
First published March 20, 2019; doi:10.1152/ajplung.00173.2018.

RESEARCH ARTICLE

Cardiac glycosides decrease influenza virus replication by inhibiting cell protein translational machinery

Luciano Amarelle,[1,2] Jeremy Katzen,[1,3] Masahiko Shigemura,[1] Lynn C. Welch,[1] Héctor Cajigas,[1] Christin Peteranderl,[4] Diego Celli,[1] Susanne Herold,[1,4] Emilia Lecuona,[1]* and Jacob I. Sznajder[1]*

[1]*Division of Pulmonary and Critical Care, Feinberg School of Medicine, Northwestern University, Chicago, Illinois;* [2]*Departamento de Fisiopatología, Hospital de Clínicas, Facultad de Medicina, Universidad de la República, Montevideo, Uruguay;* [3]*Pulmonary, Allergy, and Critical Care Division, Department of Medicine, Perelman School of Medicine, University of Pennsylvania, Philadelphia, Pennsylvania; and* [4]*Department of Internal Medicine II, University of Giessen and Marburg Lung Center, Giessen, Germany*

Submitted 20 April 2018; accepted in final form 14 March 2019

Amarelle L, Katzen J, Shigemura M, Welch LC, Cajigas H, Peteranderl C, Celli D, Herold S, Lecuona E, Sznajder JI. Cardiac glycosides decrease influenza virus replication by inhibiting cell protein translational machinery. *Am J Physiol Lung Cell Mol Physiol* 316: L1094–L1106, 2019. First published March 20, 2019; doi: 10.1152/ajplung.00173.2018.—Cardiac glycosides (CGs) are used primarily for cardiac failure and have been reported to have other effects, including inhibition of viral replication. Here we set out to study mechanisms by which CGs as inhibitors of the Na-K-ATPase decrease influenza A virus (IAV) replication in the lungs. We found that CGs inhibit influenza virus replication in alveolar epithelial cells by decreasing intracellular potassium, which in turn inhibits protein translation, independently of viral entry, mRNA transcription, and protein degradation. These effects were independent of the Src signaling pathway and intracellular calcium concentration changes. We found that short-term treatment with ouabain prevented IAV replication without cytotoxicity. Rodents express a Na-K-ATPase-α1 resistant to CGs. Thus we utilized Na-K-ATPase-α_1-sensitive mice, infected them with high doses of influenza virus, and observed a modest survival benefit when treated with ouabain. In summary, we provide evidence that the inhibition of the Na-K-ATPase by CGs decreases influenza A viral replication by modulating the cell protein translational machinery and results in a modest survival benefit in mice.

antiviral treatment; intracellular potassium; Na-K-ATPase

INTRODUCTION

Cardiac glycosides (CGs) are a family of steroidal compounds that inhibit the Na-K-ATPase and have been commonly used in the treatment of cardiac diseases (25). Although the clinical use of CGs has decreased (56), they still are used for treatment of heart failure (45) and atrial fibrillation (29). Interestingly, in the past two decades, other therapeutic effects of CGs have emerged, such as an anticancer drug (38). More recently, in vitro screenings have revealed that CGs could be potential antiviral drugs with effectiveness against influenza virus (26) and other pathogenic viruses including both RNA (3, 8, 21) and DNA viruses (18, 23, 28). CGs exert their action by binding to their receptor, Na-K-ATPase (16). Depending on the dose, CG binding to Na-K-ATPase could inhibit its function, affecting intracellular concentrations of Na^+ and K^+ ions (15, 46), or activate signal transduction pathways via the Src kinase (24, 36).

Influenza virus infection causes significant morbidity with an annual global incidence between 5 and 10% in adults and even higher in children, 3–5 million cases worldwide develop severe illness, and there are ~250,000 to 500,000 deaths per year (59a). In the 2015–2016 season, more than 10,000 deaths were reported in the United States (49). The viral cycle begins with the attachment of the virus to the host cell through the binding of the viral hemagglutinin with sialic acid of the glycoproteins or glycolipids of the cellular surface (58). Subsequently, the endocytosis and fusion of the virus with the endosomal membrane allow the release of the viral components into the cell cytoplasm via acidification of the endosome through an ionic pore formed by the viral protein matrix 2 (M2) (43). The viral RNA is replicated, transcribed to mRNA, and translated into proteins by the host cell translation machinery (35). In the final steps of the cycle, the viral proteins and RNA are transported to the plasma membrane where the budding and release of newly formed viral particles occur (40).

In the present study, we set out to study mechanisms by which CGs decrease viral replication and found that CGs, by inhibiting Na-K-ATPase, decrease the levels of intracellular potassium, which in turn inhibits the cell protein machinery and thus viral replication. Rodents are relatively insensitive to cardiac glycosides needing 1,000-fold higher concentrations than other mammals to show inhibition of Na-K-ATPase in vitro (1). However, using a lethal dose of influenza A virus (IAV) in transgenic CG-sensitive mice (20), we found that ouabain treatment moderately improved survival.

MATERIALS AND METHODS

Reagents. All cell culture reagents were from Corning Life Sciences (Tewksbury, MA), except where indicated. Alveolar Epithelial Cell Medium (no. 3201) was from ScienCell Research Laboratories (Santiago, CA). Ouabain (no. 102541) was from MP BioScience (Santa Ana, CA). Cinobufagin (no. C1272), digoxin (no. D6003), BAPTA-AM (no. A1076), valinomycin (no. V0627), pinacidil (no. P154), and chloroquine (no. C6628) were from Sigma-Aldrich (St.

* E. Lecuona and J. I. Sznajder contributed equally to this work.
Address for reprint requests and other correspondence: E. Lecuona, Pulmonary and Critical Care Medicine, 240 E. Huron St., McGaw M300, Feinberg School of Medicine, Northwestern Univ., Chicago, IL 60611 (e-mail: e-lecuona@northwestern.edu).

Louis, MO). Lactacystin (no. 426100) and PP2 (no. 529573) were from Calbiochem (San Diego, CA). MG-132 (no. 474790) from EMD Millipore (Burlington, MA). The Na/Ca exchanger inhibitor SN6 (no. 203698) was from Santa Cruz Biotechnology (Dallas, TX). Puromycin dihydrochloride (no. A1113803) was from Thermo Fisher (Waltham, MA). L-364,373 (no. 2660) was from Tocris Bioscience (Bristol, UK).

Virus and cell lines. Influenza virus strain A/WSN/1933 (WSN) was provided by Robert Lamb (Dept. of Molecular Biosciences, Northwestern University, Evanston, IL) and grown by the Cell Culture and Translational Studies Core (P01-HL-071643-12 Core B) (13). Viral titers were measured by plaque assay in Madin-Darby canine kidney (MDCK) epithelial cells. Virus aliquots were stored in liquid nitrogen, and freeze/thaw cycles were avoided. A549, BEAS-2B, and MDCK cells were from American Type Culture Collection (no. CCL 185; no. CRL-9609 and no. CCL-34 respectively; Manassas, VA). Mouse embryonic fibroblasts cells (S/S and A/A clones) were generously provided by R. Kaufman from University of Michigan (53). A549 cells stably expressing the rodent α_1-subunit isoform of Na-K-ATPase were generated as described previously (6). Human alveolar type II (ATII) cells were isolated from explanted lungs from the Northwestern Medicine Lung Transplant Program. Human pulmonary alveolar epithelial cells were purchased from ScienCell Research Laboratories (no. 3200).

Antibodies. For anti-nucleoprotein, Western blot (no. 20343) and fluorescence microscopy (no. 128193) were from Abcam (Cambridge,

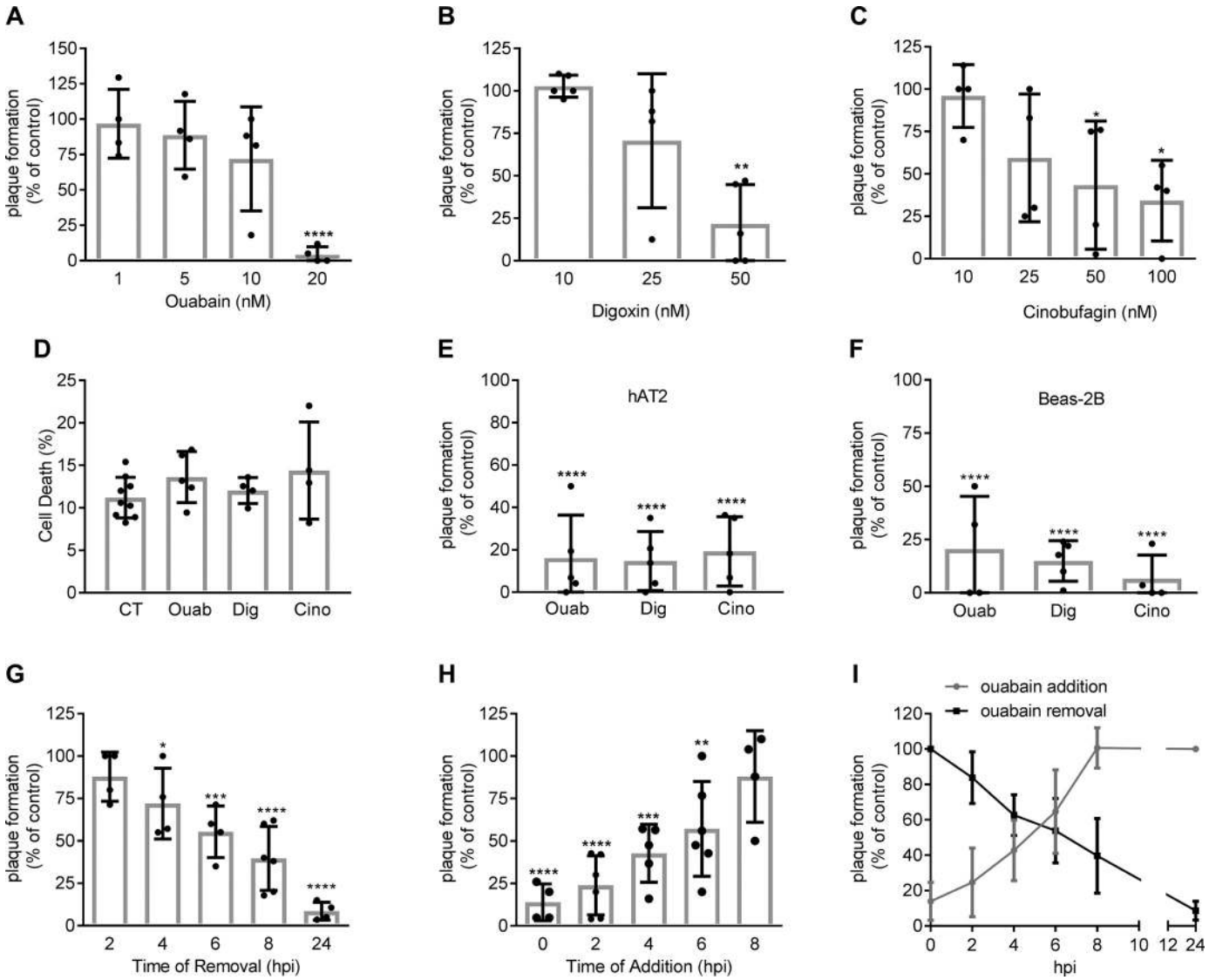

Fig. 1. Cardiac glycosides inhibit influenza A virus replication between 4 and 6 h postinfection. *A–C*: A549 cells were infected for 1 h with 1 multiplicity of infection WSN virus, washed, and treated at 0 h postinfection (hpi) with increasing concentrations of ouabain ($n = 4$; *A*), digoxin ($n = 4–5$; *B*), or cinobufagin ($n = 4$; *C*). Twenty-four hpi virus titer was determined by plaque assay of the supernatant. *D*: A549 cells were treated for 24 h with PBS (CT; $n = 9$), 20 nM ouabain (Ouab; $n = 5$), 50 nM digoxin (Dig; $n = 4$), or 100 nM cinobufagin (Cino; $n = 4$), and cell death was measured using LDH assay. *E*: human primary human alveolar type II (ATII) cells were infected as in *A*; treated at 0 hpi with 20 nM ouabain, 50 nM digoxin, or 100 nM cinobufagin; and 24 hpi virus titer was measured via plaque assay ($n = 5$). *F*: human BEAS-2B cells were infected as in *A*; treated at 0 hpi with 20 nM ouabain, 50 nM digoxin, or 100 nM cinobufagin; and 24 hpi virus titer was measured via plaque assay ($n = 4–5$). *G*: time of removal of A549 cells infected as in *A* and treated 0 hpi with 20 nM ouabain. Ouabain was removed from the media at 2-h intervals, from 0 to 24 hpi. Twenty-four hpi virus titer was measured via plaque assay ($n = 4–6$). *H*: time of addition of A549 cells infected as in *A* and treated with 20 nM ouabain at 2-h intervals [from 0 to 8 hpi]. Twenty-four hpi, virus titer was measured via plaque assay ($n = 4–6$). *I*: viral titers were plotted as a function of time-of-addition and time-of-removal. All graphs show means ± SD. Graphs were analyzed by one-way ANOVA with Dunnett's post hoc test. $^*P < 0.05$, $^{**}P < 0.01$, $^{***}P < 0.001$, $^{****}P < 0.0001$.

UK). Anti-Matrix 1 (no. 22396) was from Abcam. Anti-nonstructural 1 (no. 130568), and anti-β-tubulin (H-235) (no. 9104) were from Santa Cruz Biotechnology. Anti-actin (no. 2066) was from Sigma-Aldrich. Anti-Stat3 (no. 12640), anti-phospho-eukaryotic initiation factor 2α (eIF2α; no. 9721), anti-total-eukaryotic initiation factor-2α (no. 2103), and anti-GADPH (D16H11) (no. 5174) were from Cell Signaling (Danvers, MA). Anti-Puromycin (no. MABE341) was from EMD Millipore. Goat anti-rat IgG-HPR (no. 2006) was from Santa Cruz Biotechnology. Goat anti-mouse IgG HPR (no. 1721011) and goat anti-rabbit IgG HPR (no. 1706515) were from Bio-Rad (Hercules, CA). Goat anti-mouse Alexa fluor 568 (no. A11004) was from Life Technologies (Carlsbad, CA).

PCR primers. Primers for nucleoprotein (NP), matrix 1 (M1), and GADPH were purchased from Integrated DNA Technologies (Coralville, IA). Sequences were as follows: M1 forward: 5′-GAC-CAA-TCC-TGT-CAC-CTC-3′; M1 reverse: 5′-GAT-CTC-CGT-TTC-CAT-TAA-GAG-3′; NP forward: 5′-CTC-GTC-GCT-TAT-GAC-AAA-GAA-3′; NP reverse: 5′-AGA-TCA-TCA-TGT-GAG-

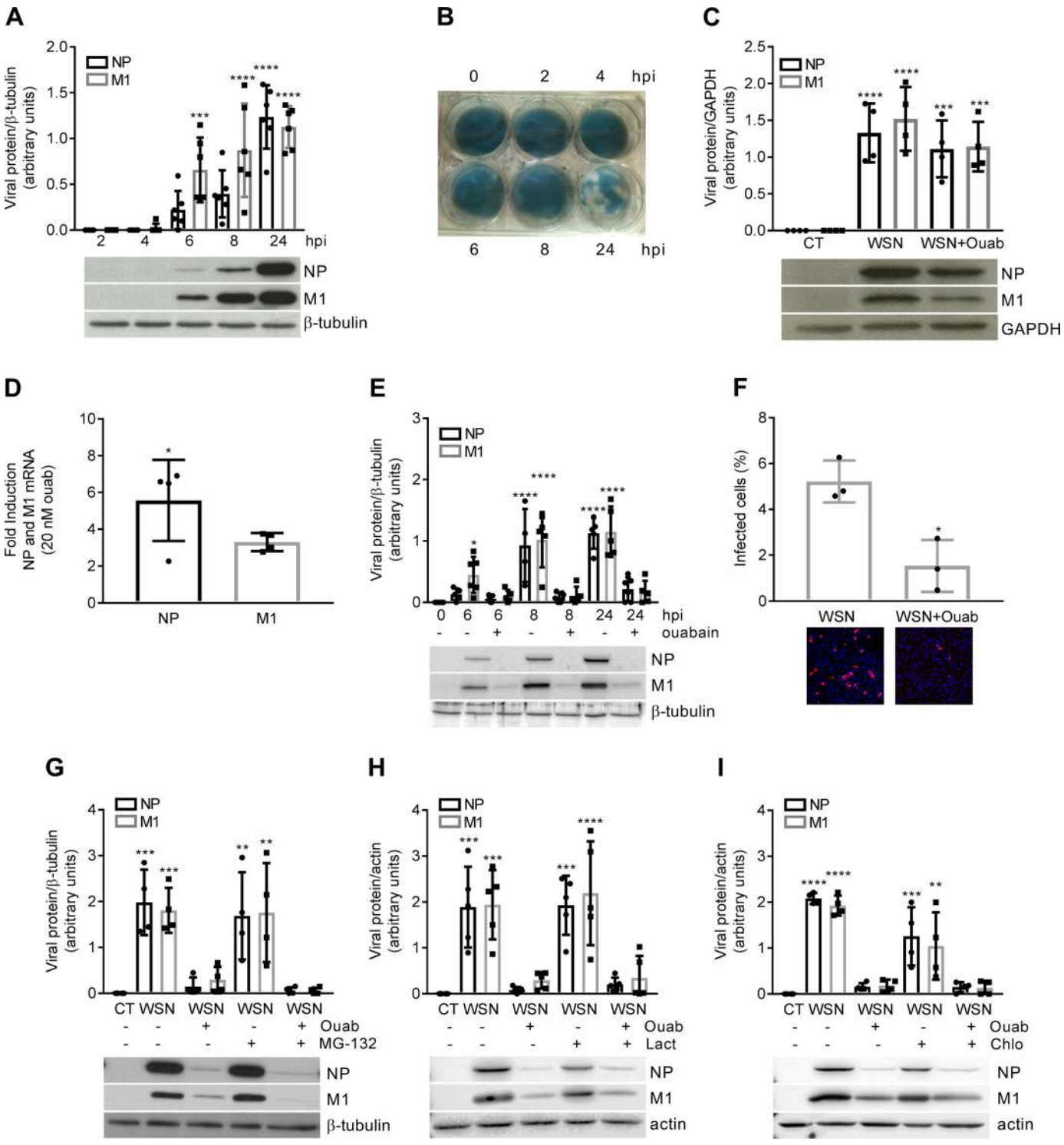

TCA-GAC-3′; GADPH forward 5′-ACC-ACA-GTC-CAT-GCC-ATC-AC-3′; and GADPH reverse 5′-TCC-ACC-ACC-CTG-TTG-CTG-TA-3′.

Mice. Ouabain Na-K-ATPase-α_1-sensitive mice ($^{S/S}$mice):R111Q mutant mice were mated for over 10 generations onto C57BL/6 mice and were generously provided to us by J. Lingrel (Univ. of Cincinnati, Cincinnati, OH; Ref. 20) and housed at the Center of Comparative Medicine at Northwestern University.

Cell culture and in vitro infections. Cells were cultured in DMEM supplemented with 20 mM HEPES buffer, 10% fetal bovine serum (FBS), 100 U/ml penicillin, and 100 μg/ml streptomycin. Cells were seeded in 12-well plates to a single confluent monolayer and 24 h later inoculated with IAV at 1 multiplicity of infection (MOI = 1) in infection media: DMEM + 0.1% FBS + 0.3% bovine serum albumin (BSA) in a humidified atmosphere of 5% CO_2-95% air at 37°C. For alkalemic conditions, medium without potassium was made with sterile H_2O, 6,400 mg/l NaCl, 200 mg/l $CaCl_2$, 97.7 mg/l $MgSO_4$, 125 mg/l Na_2HPO_4, 3,700 mg/l $NaHCO_3$, 4,500 mg/l D-glucose, 10 ml HEPES, 0.1% FBS, 100 U/ml penicillin, and 100 μg/ml streptomycin. For single-cycle infection experiments, after 1 h, cells were washed and infection medium was replaced, and then, the assigned drug was added for the desired time and cells were lysed with cell lysis buffer (Cell Signaling) for Western blot analysis or RNA was extracted for real-time quantitative polymerase chain reaction (qPCR). For multicycle infection, cells were infected and the drug was added 1 h later without washing of the media.

Plaque assays. The supernatant of infected cells was collected at the indicated time points postinfection and centrifuged at 2,000 rpm, and the supernatant was frozen at −80°C until assay day. Lungs of infected mice were collected at the indicated times, homogenized, and kept at −80°C until assay day as described before (39). MDCK cells were grown in six-well plates, incubated with a 10-fold serially diluted supernatant for 1 h in DMEM with 1% BSA at 37°C and 5% CO_2 atmosphere, washed with phosphate-buffered saline (PBS) buffer and replacement media with DMEM, and 2.7% avicel (FBC Biopolymer no. RC-591NF), and 1.5 μg/ml of *N*-acetyl trypsin were added. After 3 days of incubation, the overlay was removed and viral plaques were visualized using naphthalene black dye solution (0.1% naphthalene black, 6% glacial acetic acid, and 1.36% anhydrous sodium acetate). Viral titer (plaque-forming units/ml) was calculated as number of plaques/(dilution factor) × (inoculum per well), as described elsewhere (27). For in vivo experiments, whole lungs were homogenized in PBS and placed on ice immediately until use for plaque assay.

Cell death assay. To measure cell death, LDH assay was performed using the Roche Cytotoxicity Detection Kit (no. 11644793001).

Western blot analysis. Protein concentration was quantified from cell lysates by Bradford assay (Bio-Rad), and proteins were resolved in 10–15% polyacrylamide gels. Thereafter, proteins were transferred to nitrocellulose membranes (Bio-Rad) using a Trans Blot Turbo (Bio-Rad). Incubation with specific antibodies was performed overnight at 4°C. Blots were developed with a chemiluminescence detection kit (Perkin Elmer), and the bands were visualized with an Odyssey FC Imager using Image Studio Software (LI-COR, Lincoln, NE).

Real-time qPCR. Total RNA was extracted using miRNeasy Mini kit (Qiagen). cDNA was synthesized from 1 μg of total RNA by using a qScript cDNA Synthesis kit (Quanta Biosciences, Beverly, MA), and mRNA expression was determined by qPCR using SYBR Green chemistry (Bio-Rad). Relative expression of the transcripts was determined according to the ΔΔCt method using GADPH as reference for normalization.

Time of addition and removal. At the time of addition, A549 cells were infected and then treated with 20 nM ouabain at 2-h intervals [from 0 hours postinfection (hpi) to 8 hpi]. For time of removal, A549 cells were infected and then treated with 20 nM ouabain at time 0 hpi. At 2-h intervals, ouabain was removed from the growth media, from 0 to 24 hpi. After 24 h, virus titer was measured via plaque assay.

Immunocytochemistry. A549 cells were single or multicycle infected with WSN virus at 1MOI and treated with 20 nM ouabain and fixed, permeabilized, and stained with NP antibody. Nuclei were visualized by Hoechst 33342 (no. H3570; Invitrogen, Carlsbad, CA). Pictures were acquired using Axioplan 2 imaging fluorescent microscopy (Carl Zeiss).

Global protein synthesis assay. For determining global protein synthesis with surface sensing of translation (SUnSET) assay, cells were incubated 30 min with puromycin 20 μM before cell lysis and specific anti-puromycin antibodies were used (54).

Measurement of intracellular Na^+ and K^+. Intracellular K^+ was measured by Thermo iCAP Q Inductively Coupled Plasma Mass Spectrometry at the Northwestern University Quantitative Bio-element Imaging Center generously supported by NASA Ames Research Center NNA06CB93G. Intracellular Na^+ was measured with the fluorescent Na^+ indicator CoroNa green AM (no. C36676; Thermo Fisher Scientific). Briefly, after treatment with ouabain, cells were incubated 30 min with 5 μM CoroNa green and washed with PBS and fluorescence was measured at excitation 492 nm and emission 516 nm using Gemini EM Microplate Reader (Molecular Devices, Sunnyvale, CA).

Precision-cut lung slices and ex vivo infection. Lungs of $^{S/S}$mice were excised for precision-cut lung slices. Briefly, following tracheotomy, excised mouse lungs were insufflated with 2.5% low-melting point agarose in PBS and placed in cold PBS, and after the agarose gelled, the right lobe was separated and sectioned into slices 100 μm thick using a tissue slicer (Precisionary Instruments VF-300). Lung slices were incubated at 37°C in DMEM supplemented with 10% FBS, 100 U/ml penicillin, and 100 μg/ml streptomycin in 24-well plates. After 1 h, the slices were washed, 1 ml of infection media was added and 2.5×10^6 WSN virus was instilled; at 1 hpi, 20 nM ouabain was added to the assigned wells; and then at 24 hpi, ouabain was quenched using 20 mM KCl. After 0, 24, and 48 h postouabain, the

Fig. 2. Cardiac glycosides inhibit influenza A virus replication by impairing protein translation. *A*: A549 cells were infected for 1 h with 1 multiplicity of infection WSN and lysed at 2, 4, 6, 8, and 24 h postinfection (hpi), and protein expression was analyzed by Western blotting. Viral proteins nucleoprotein (NP) and matrix 1 (M1) were detected using specific antibodies. Graph represents viral protein abundance relative to the internal control (β-tubulin) ($n = 6$). *B*: representative image of a viral plaque assay from supernatant collected from A549 cells infected as in *A* and collected 0, 2, 4, 6, 8, and 24 hpi ($n = 4$). *C*: A549 cells were preincubated for 2 h with 20 nM ouabain (Ouab), washed, infected as in *A*, and lysed at 24 hpi for Western blot analysis of viral proteins NP and M1. Graph represents viral protein abundance relative to the internal control (CT; GAPDH) ($n = 4$). *D*: A549 cells were infected as in *A*, PBS or 20 nM ouabain was added at 0 hpi, and NP and M1 mRNA abundance was quantified by quantitative PCR at 24 hpi. Graph represents fold change of viral mRNA of infected cells vs. infected cells treated with ouabain ($n = 4$). *E*: A549 cells were infected as in *A*, and 20 nM ouabain was added at 0 hpi. Cells were lysed at 0, 6, 8, and 24 hpi, and viral proteins NP and M1 were detected by Western blotting using specific antibodies. Graph represents viral protein abundance relative to the internal control (β-tubulin) ($n = 4–6$). *F*: A549 cells were infected as in *A*, 20 nM ouabain was added at 0 hpi, and 24 hpi cells were fixed and NP (red) and nuclei (blue) were analyzed by immunofluorescence microscopy. Graph represents quantification of infected cells analyzed by unpaired *t*-test ($n = 3$). *G–I*: A549 cells were infected as in *A* and then treated at 0 hpi with 20 nM ouabain in the presence or absence of 1 μM MG-132 (*G*), 1 μM lactacystin (Lact; *H*), and 10 μM chloroquine (Chlo; *I*). At 8 hpi, cells were lysed and proteins were detected by Western blotting using specific antibodies. Graphs represent viral protein abundance relative to the internal control (β-tubulin or actin) ($n = 4–5$). All graphs show means ± SD. Except for *F*, graphs were analyzed by one-way ANOVA with Dunnett's post hoc test. $^*P < 0.05$, $^{**}P < 0.01$, $^{***}P < 0.001$, $^{****}P < 0.0001$.

tissue was fixed in 3.7% paraformaldehyde, permeabilized with 0.1% TritonX-100 5 min at room temperature, washed and blocked in normal goat serum + 0.2% BSA at 37°C for 1 h, washed once with PBS and incubated with primary NP antibody overnight at 37°C, and washed with PBS and incubated with secondary antibody goat anti mouse Alexa fluor 568 and then with 1 μg/ml Hoechst 33342 (no. H3570; Invitrogen) for nucleic acid staining. Slices were mounted in glass microslides with fluoromount mounting media (no. F4680; Sigma-Aldrich) and stored in the dark at room temperature overnight. With the use of the same protocol as per ex vivo immunostaining, slices were analyzed using ImageJ 1.48 v (National Institutes of Health).

In vivo experiments. The $^{S/S}$mice, males and females between 9 and 12 wk of age and weighing 20–25 g, were infected with WSN IAV by intratracheal instillation under inhalation anesthesia with isoflurane as described elsewhere (39) with a lethal doses of IAV. The mice were treated with 50 μg/kg ouabain or saline solution by intraperitoneal injection beginning the infection day, daily for 2 days. For the mortality curve, mice were followed for up to 15 days after infection, weight was recorded daily, and mortality was recorded up to three times a day.

Ethics statement. Animal work was conducted in accordance with the recommendations in the *Guide for the Care and Use of Laboratory Animals* of the National Institutes of Health. All animals were provided with food and water ad libitum, maintained on a 14-h light/10-h dark cycle, and handled according to National Institutes of Health guidelines. All procedures were approved and conducted according to regulations of the Northwestern University Institutional Animal Care and Use Committee (protocol no. IS00000380). Intratracheal instillation of IAV was performed under anesthesia with isoflurane. Human alveolar type II (ATII) cells were isolated by the Cell Culture and Translational Studies Core (P01-HL-071643-12 Core B) from explanted lungs provided by the National Disease Research Interchange. The use of human lung samples was approved by the Institutional Review Board Office of Northwestern University (no. STU00041428-CR0001). All samples were anonymized. Human data collection was approved by the Northwestern University Institutional Review Board (no. SA1707).

Statistical analysis. Data are expressed as means ± SD. For comparisons between two groups, significance was evaluated by unpaired Student's *t*-test. When more than two groups were compared, one-way ANOVA was used followed by the Dunnett's or Sidak's post hoc test. Mortality curves were compared by log-rank (Mantel-Cox) test using GraphPad Prism 7.02 software.

RESULTS

Cardiac glycosides inhibit IAV replication. To determine the minimal effective dose of CGs against influenza A virus (IAV) and whether all CGs have the same effect, we exposed the human cell line A549 to increasing concentrations of ouabain and digoxin (cardenolides) or cinobufagin (bufadenolides) (46). We observed that the minimal dose necessary to inhibit IAV replication without cytotoxic effect at 24 h post infection (hpi) was 20 nM for ouabain, 50 nM for digoxin, and 100 nM for cinobufagin (Fig. 1, *A–D*). An inhibitory effect on IAV replication was also observed in primary human alveolar epithelial cells as well as in the bronchial epithelial cell line BEAS-2B (Fig. 1, *E* and *F*). To determine the time of action of ouabain in the viral cycle, we performed time-of-addition and time-of-removal experiments and determined viral replication by plaque assay. We observed that at least 4 h of incubation with ouabain after infection was needed to inhibit IAV replication and that the inhibitory effect decreases if the drug was added later than 6 hpi (Fig. 1, *G–I*). Together, these data suggest that CGs inhibit IAV replication between 4 and 6 hpi of the viral cycle.

Cardiac glycosides inhibit IAV replication by impairing protein translation. To explore which viral processes occur between 4 and 6 hpi in our in vitro study conditions, we first determined that viral proteins are translated between 4 and 6 hpi (Fig. 2*A*). Virus budding occurred between 8 and 24 hpi (Fig. 2*B*), suggesting that ouabain acts between the virus entry and protein translation. To determine whether ouabain affected the early steps in the viral cycle, attachment and endocytosis, we incubated A549 cells for 2 h with 20 nM ouabain before IAV infection and found that preincubation with ouabain did not affect IAV replication (Fig. 2*C*). As virus entry was not affected by ouabain, we assessed whether the transcription of viral mRNA was regulated by ouabain treatment. We performed qPCR for IAV mRNA using specific primers and found that viral mRNA expression was not decreased after ouabain treatment (Fig. 2*D*). We observed by Western blotting and immunofluorescence decreased viral protein abundance after ouabain treatment (Fig. 2, *E* and *F*), which was independent of protein degradation, as pharmacological inhibition of the pro-

Fig. 3. Na-K-ATPase inhibition shuts off the translational machinery via intracellular ionic changes and independently of eukaryotic initiation factor 2α (eIF2α) phosphorylation. *A*: A549 cells were treated with 20 nM ouabain for 0, 2, 4, 6, and 8 h. Cells were lysed at those time points, and phospho-eIF2α and total-eIF2α were detected by Western blotting using specific antibodies. Graph represents phospho- vs. total-eIF2α ($n = 4–6$). *B*: mouse embryonic fibroblast (MEF) cells expressing wild-type (WT) eIF2α (clone S/S) were infected as in *A* and treated at 0 h postinfection (hpi) with 100 μM ouabain (Ouab). At 24 hpi, proteins were lysed and viral nucleoprotein (NP) and matrix 1 (M1) proteins were detected by Western blotting using specific antibodies. Graph represents viral protein abundance relative to the internal control (CT; actin) ($n = 4$). *C*: mouse embryonic fibroblasts cells expressing S51A eIF2α (clone A/A) were infected as in *A* and treated at 0 hpi with 100 μM ouabain. At 24 hpi, proteins were lysed and viral NP and M1 proteins were detected by Western blotting using specific antibodies. Graph represents viral protein abundance relative to the internal control (β-tubulin) ($n = 4$). *D*: A549 cells were infected as in *A*, and at 0 hpi 20 nM ouabain was added in the presence or absence of 10 μM of the Src inhibitor PP2. At 8 hpi, proteins were lysed and viral proteins M1 and NS1 were detected by Western blotting using specific antibodies. Graph represents viral protein abundance relative to the internal control (actin) ($n = 3$). *E*: A549 cells were infected as in *A* and 0 hpi media were replaced with 5 mM KCl or 0 mM KCl media. At 24, hpi cells were lysed and viral proteins NP and M1 were detected by Western blotting using specific antibodies. Graph represents viral protein abundance relative to the internal control (actin) ($n = 4–5$). *F*: A549 cells expressing the Na-K-ATPase rat α_1-subunit were infected as in *A*, and 20 nM ouabain was added at 0 hpi. At 8 hpi, cells were lysed and viral proteins NP and NS1 detected by Western blotting using specific antibodies. Graph represents viral protein abundance relative to the internal control (actin) ($n = 5$). *G* and *H*: A549 cells were treated with 20 nM ouabain for 2, 4, or 6 h, and intracellular potassium concentration was measured by inductively coupled plasma/mass spectrometry ($n = 6–7$; *G*) and intracellular sodium concentration by fluorescence assay ($n = 5$; *H*). *I* and *J*: A549 cells were infected as in *A*, and at 0 hpi 20 nM ouabain was added in the presence or absence of 10 μM of Na^+/Ca^{2+} exchanger SN-6 (*I*) or 25 μM of calcium chelator BAPTA-AM (*J*). Viral proteins NP and NS1 were detected by Western blotting using specific antibodies. Graphs represent viral protein abundance relative to the internal control (actin) ($n = 3–5$). All graphs show means ± SD. Graphs were analyzed by one-way ANOVA with Dunnett's post hoc test. $^*P < 0.05$, $^{**}P < 0.01$, $^{***}P < 0.001$, $^{****}P < 0.0001$.

teasomal and lysosomal systems did not blunt the effect of ouabain (Fig. 2, *G–I*). Taken together these data suggest that ouabain impairs IAV replication by inhibiting viral protein translation.

Na-K-ATPase inhibition shuts off the translational machinery via intracellular ionic changes and independently of eIF2α phosphorylation. Mammalian cells respond to viral infections through activation of dsRNA-dependent protein kinase (PKR),

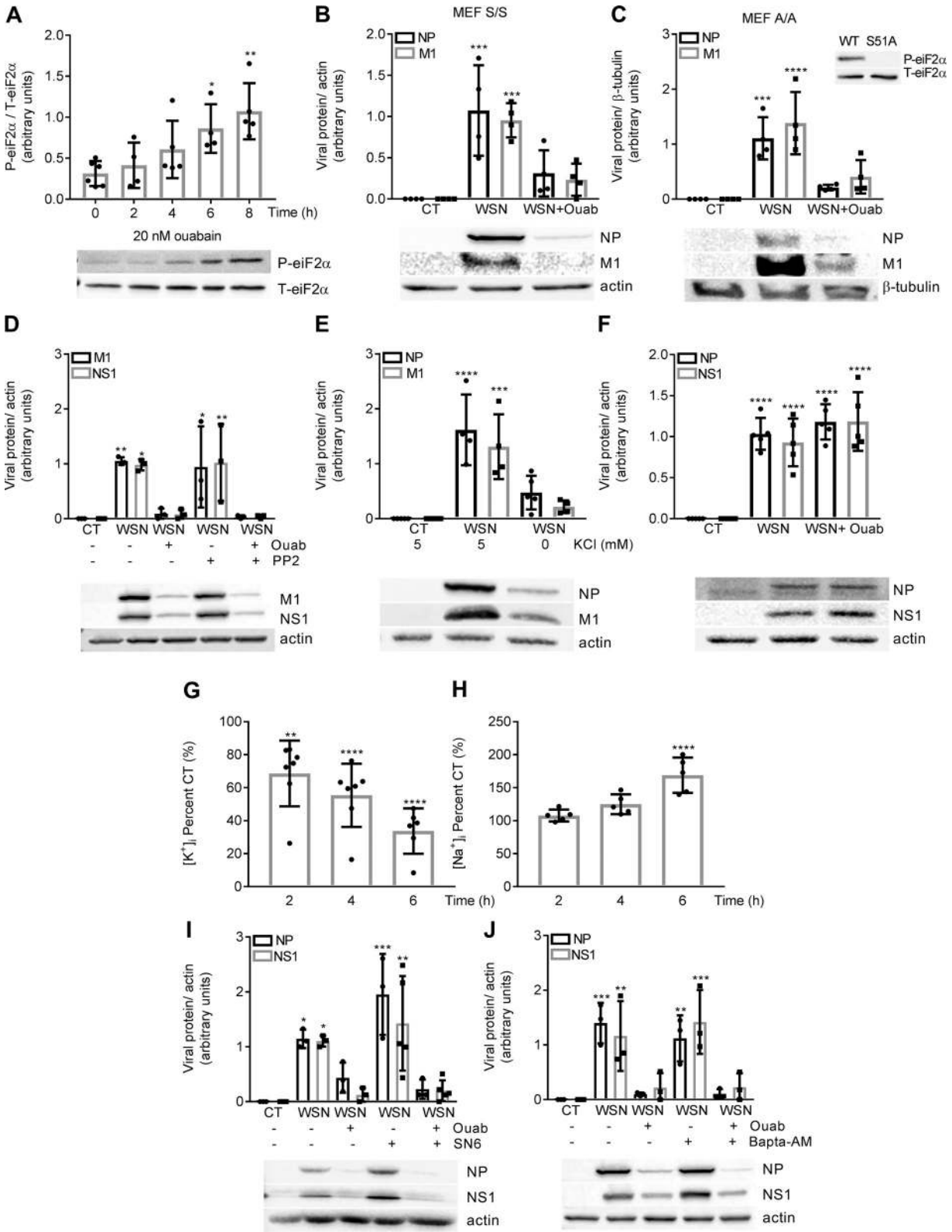

which phosphorylates the eukaryotic translation initiation factor 2α subunit (eIF2α) leading to inhibition of protein synthesis from viral mRNAs (17, 48). However, IAV hijacks the host cell machinery preventing eIF2α phosphorylation and favors its own replication (37, 44). We explored whether ouabain counteracted the effect of IAV on eIF2α phosphorylation and thus inhibits IAV replication and found that cells treated with ouabain had increased eIF2α phosphorylation (Fig. 3*A*). To determine whether phosphorylation of eIF2α played a role in the inhibition of viral protein synthesis by ouabain, we incubated mouse embryonic fibroblasts constitutively expressing wild-type eIF2α (clone S/S) or eIF2α where Ser51 was substituted for an alanine (S51A) (clone A/A; which cannot be phosphorylated) (53), with ouabain after IAV infection and found decreased IAV replication in both wild-type and S51A, suggesting that the anti-influenza action of ouabain is independent of eIF2α phosphorylation (Fig. 3, *B* and *C*).

It is known that the binding of ouabain to the Na-K-ATPase not only inhibits the transport of sodium and potassium ions across the plasma membrane but also activates intracellular signaling pathways through Src kinase (36). We explored both ionic and signaling pathways and found that inhibition of Src did not alter the decreased IAV replication induced by ouabain (Fig. 3*D*). To assess in a different way whether inhibiton of the Na-K-ATPase affects IAV replication, we incubated A549 cells with media without extracellular potassium (41) and observed inhibition of IAV replication, which was similar to our results with ouabain (Fig. 3*E*). Taking advantage of the fact that rodents are resistant to CGs needing higher doses to get the same inhibition (33), we used A549 cells expressing a resistant rodent Na-K-ATPase α_1-subunit (6) and found that 20 nM ouabain treatment did not have an effect on IAV replication in (Fig. 3*F*). These findings suggest that the effect of ouabain on IAV replication was due to inhibition of Na-K-ATPase activity.

To study the effect of 20 nM ouabain in the concentration of intracellular ions, we measured intracellular Na^+ concentration ($[Na^+]_i$) and intracellular K^+ concentration ($[K^+]_i$) and showed a significant decrease in $[K^+]_i$ as early as 2 h after ouabain treatment (Fig. 3*G*), while $[Na^+]_i$ increased after 6 h (Fig. 3*H*). It has been described that an increase in $[Na^+]_i$ could lead to a consequential increase in intracellular Ca^{2+} concentration ($[Ca^{2+}]_i$) (47). Therefore, we studied whether $[Ca^{2+}]_i$ changes were responsible for the effect of ouabain on IAV replication. We found that neither pharmacological inhibition of the Na^+-Ca^{2+} exchanger with 10 μM of the selective inhibitor SN-6 (Fig. 3*I*) nor incubation with 25 μM the calcium chelator BAPTA-AM (Fig. 3*J*) blunted the effect of ouabain in IAV protein translation, suggesting that $[Ca^{2+}]_i$ changes are not involved in the effect of ouabain on IAV replication.

Na-K-ATPase inhibition shuts off the protein translational machinery via decreased intracellular potassium. Since potassium is required for normal protein synthesis (4), and we found a profound decrease in $[K^+]_i$ in cells incubated with 20 nM ouabain (Fig. 3*G*), we assessed whether inhibition of Na-K-ATPase activity had an effect in protein synthesis. Figure 4, *A* and *B* , shows that a 24-h incubation with either 20 nM ouabain or 0 mM KCl led to inhibition of global protein synthesis assessed by SUnSET (54) (Fig. 4*A*) and confirmed by the decreased expression of STAT3 [half-life ~8.5 h (55)] and no change in T-eiF2α [half-life ~10 days (22)] (Fig. 4*B*). To confirm that the effect of CGs in the virus replication is through the decrease in $[K^+]_i$, we utilized a pharmacological approach using three different drugs that decrease $[K^+]_i$ levels: the ionophore valinomycin (50) (Fig. 4, *C* and *D*), the voltage-dependent potassium channel activator L_364, 373 (52) (Fig. 4, *E* and *F*), and the calcium-dependent potassium channel activator pinacidil (5) (Fig. 4, *G* and *H*). All three showed a dose-dependent decrease in viral protein translation, as well as cellular global protein synthesis.

Short-term inhibition of protein synthesis prevents viral replication in vitro and ex vivo. Due to the global effect of ouabain in protein synthesis, we decided to explore whether short-term treatment would be effective without causing significant cytotoxicity. To examine whether the effect of ouabain was reversible, we incubated A549 cells for 24 h with ouabain, removed it from the media and determined protein synthesis 24 h postouabain removal. We found that global protein synthesis was improved (Fig. 5*A*) and that viral protein expression was still inhibited (Fig. 5*B*), suggesting that short-term treatment with ouabain could be potentially useful. Next, we explored whether ouabain had effect on a multicycle infection. To achieve short-term exposure to ouabain without removing the media in a multicycle infection, we counteracted the effect of ouabain by adding 20 mM KCl to the culture (12) (Fig. 5*C*). We found that using multicycle infection and counteracting the effect the ouabain after 24 h treatment there was a strong inhibition of viral protein expression even after 48 h post-ouabain removal (Fig. 5*D*), without significant effect on cell viability (Fig. 5*E*). To study whether short-term treatment with ouabain prevents IAV replication in an ex vivo model, we infected mouse lung precision cut slices from Na-K-ATPase-α_1-sensitive mice ($^{S/S}$mice) (20) with 2.5×10^6 plaque-forming units IAV, incubated with ouabain for 24 h and then with

Fig. 4. Na-K-ATPase inhibition shuts off the protein translational machinery via decreased intracellular potassium. *A* and *B*: A549 cells were treated with 20 nM ouabain (Ouab) or media replaced with 0 mM KCl for 24 h. *A* and *B*: surface sensing of translation (SUnSET) assay was used to visualize global protein biosynthesis (*A*), and STAT3 and T-eukaryotic initiation factor 2α (eIF2α) were detected by Western blotting (*B*) using specific antibodies. Graphs represent protein abundance relative to the internal control (CT; actin) ($n = 3$–4). *C* and *D*: A549 cells were infected for 1 h with 1 multiplicity of infection (MOI) WSN and treated at 0 hpi with increasing concentrations of valinomycin. *C* and *D*: SUnSET assay was used to visualize global protein biosynthesis (*C*) and viral proteins NP and NS1 were detected by Western blotting (*D*) using specific antibodies. Graphs represent viral protein abundance relative to the internal control (actin) ($n = 3$–4). *E* and *F*: A549 cells were infected for 1 h with 1 multiplicity of infection WSN and treated at 0 hpi with increasing concentrations of L_364. *E* and *F*: SUnSET assay was used to visualize global protein biosynthesis (*E*) and viral proteins M1 and NS1 were detected by Western blotting (*F*) using specific antibodies. Graphs represent viral protein abundance relative to the internal control (actin) ($n = 3$–4). *G* and *H*: A549 cells were infected for 1 h with 1 MOI WSN and treated at 0 hpi with increasing concentrations of pinacidil. *G* and *H*: SUnSET assay was used to visualize global protein biosynthesis (*G*) and viral proteins NP and NS1 were detected by Western blotting (*H*) using specific antibodies. Graphs represent viral protein abundance relative to the internal control (actin) ($n = 3$–4). All graphs show means ± SD. Graphs were analyzed by one-way ANOVA with Dunnett's post hoc test. $^*P < 0.05$, $^{**}P < 0.01$, $^{***}P < 0.001$, $^{****}P < 0.0001$.

20 mM extracellular KCl, and followed the replication of IAV by immunofluorescence staining for NP viral protein up to 72 h postouabain. We showed that 24 h of incubation with ouabain was effective in preventing IAV replication in lung tissue slices, and that the effect persisted for 48 h postouabain (Fig. 5, *F* and *G*).

CG effects in vivo. To determine whether ouabain has a pharmacological effect in vivo, we first infected $^{S/S}$mice via intratracheal instillation with high dose of IAV and treated the mice for 2 days with 50 $\mu g \cdot kg^{-1} \cdot day^{-1}$ ouabain by intraperitoneal injections, which was the maximal dose without toxicity (Fig. 6*A*), and found a delayed mortality

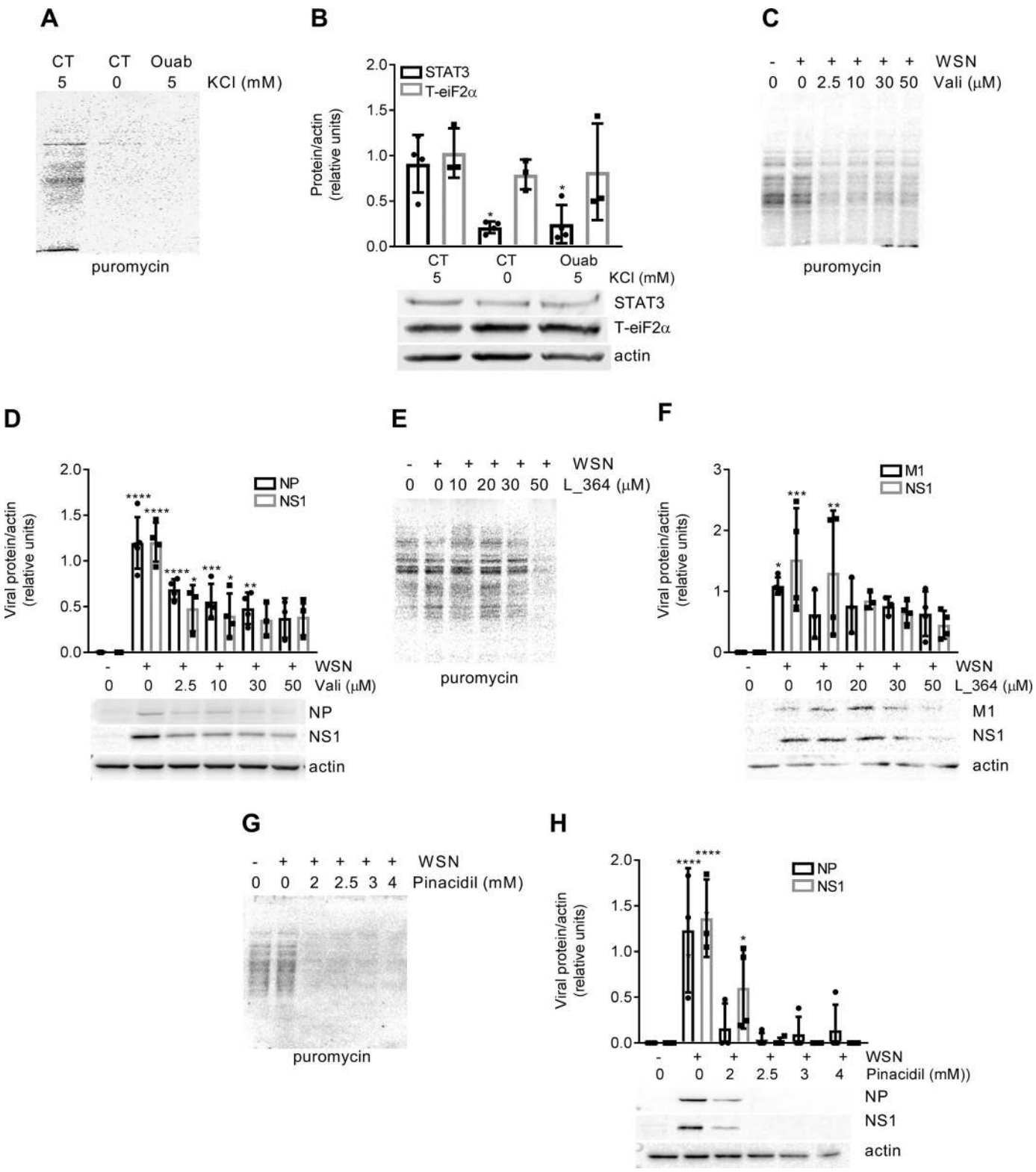

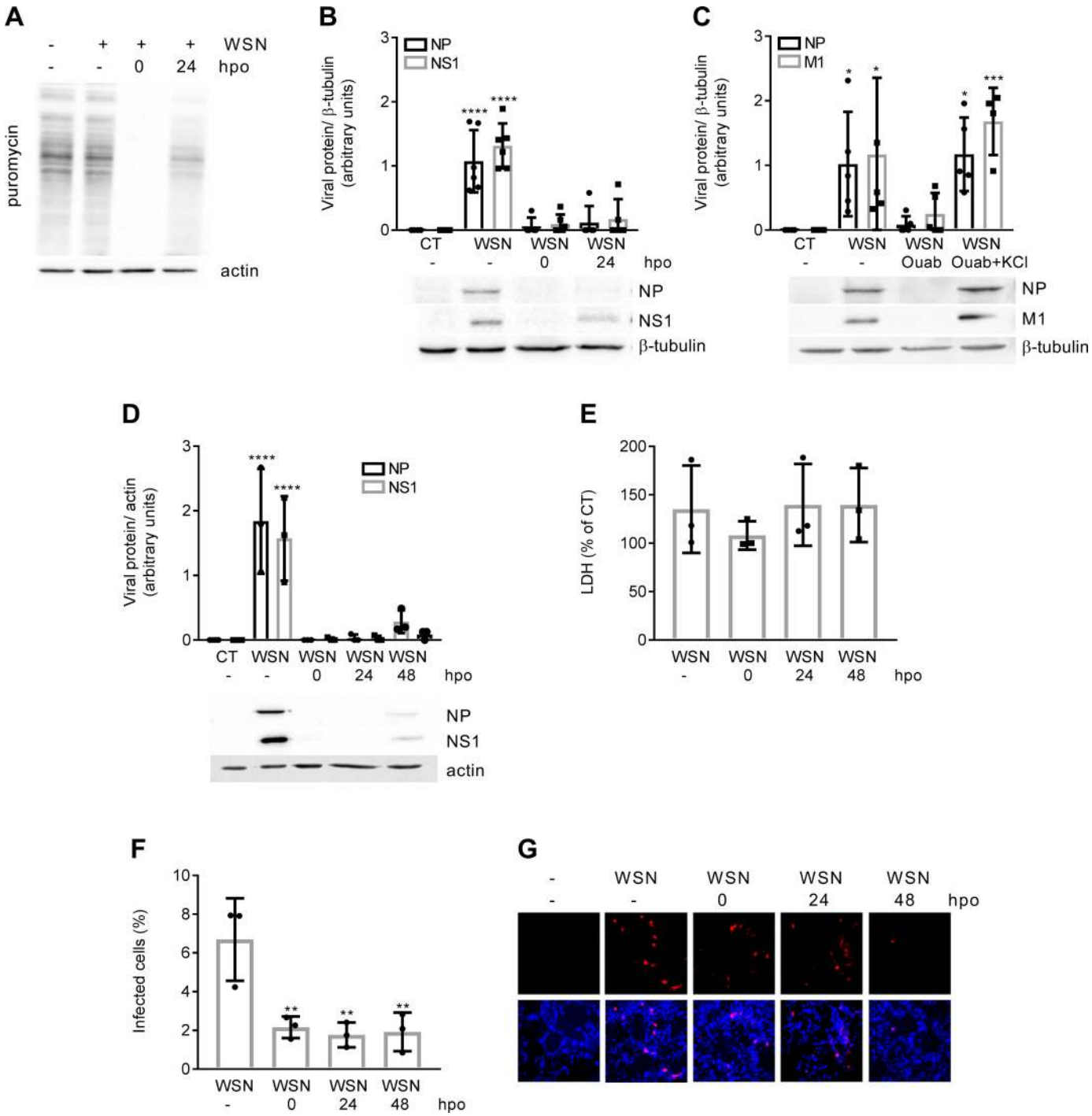

Fig. 5. Short-term inhibition of protein synthesis prevents viral replication in vitro and ex vivo. *A* and *B*: A549 cells were infected for 1 h with 1 multiplicity of infection (MOI) WSN, treated with 20 nM ouabain (Ouab) for 24 h, washed, and lysed at 0 or 24 h postouabain exposure (hpo). *A* and *B*: surface sensing of translation (SUnSET) assay was used to visualize global protein biosynthesis (*A*), and STAT3 and viral nucleoprotein (NP) and NS1 were detected by Western blotting (*B*) using specific antibodies. Graph represents viral protein abundance relative to the internal control (CT; β-tubulin) (n = 5–6). *C*: A549 cells were infected as in *A* and treated with 20 nM ouabain in the presence or absence of 20 mM KCl media for 24 h. Viral proteins NP and matrix 1 (M1) were detected by Western blotting using specific antibodies. Graph represents viral protein abundance relative to the internal control (β-tubulin) (n = 4–5). *D*: A549 cells were infected with 1 MOI WSN in a multicycle infection and treated with 20 nM ouabain for 24 h. Twenty micromolar KCl was used to counteract the effect of ouabain. Cells were washed and lysed at 0, 24, or 48 hpo and 24 hours postinfection (hpi) for the infected control. Viral proteins were detected by Western blotting using specific antibodies. Graph represents viral protein abundance relative to the internal control (actin) (n = 3). *E*: LDH assay was performed for the same conditions as in *D* (n = 3). *F* and *G*: $^{S/S}$mice lungs were cut in 100-μm slices, exposed to multicycle infection with WSN, and treated in the presence or absence of 20 nM ouabain. Incubation with 20 mM KCl was performed for 0, 24, or 48 h. Tissue was fixed and stained for immunofluorescence microscopy. *F*: graph represents quantification of infected cells (n = 3). *G*: NP viral protein (red) and nuclei (blue) were visualized. All graphs show means ± SD. Graphs were analyzed by one-way ANOVA with Dunnett's post hoc test. *$P < 0.05$, **$P < 0.01$, ***$P < 0.001$, ****$P < 0.0001$.

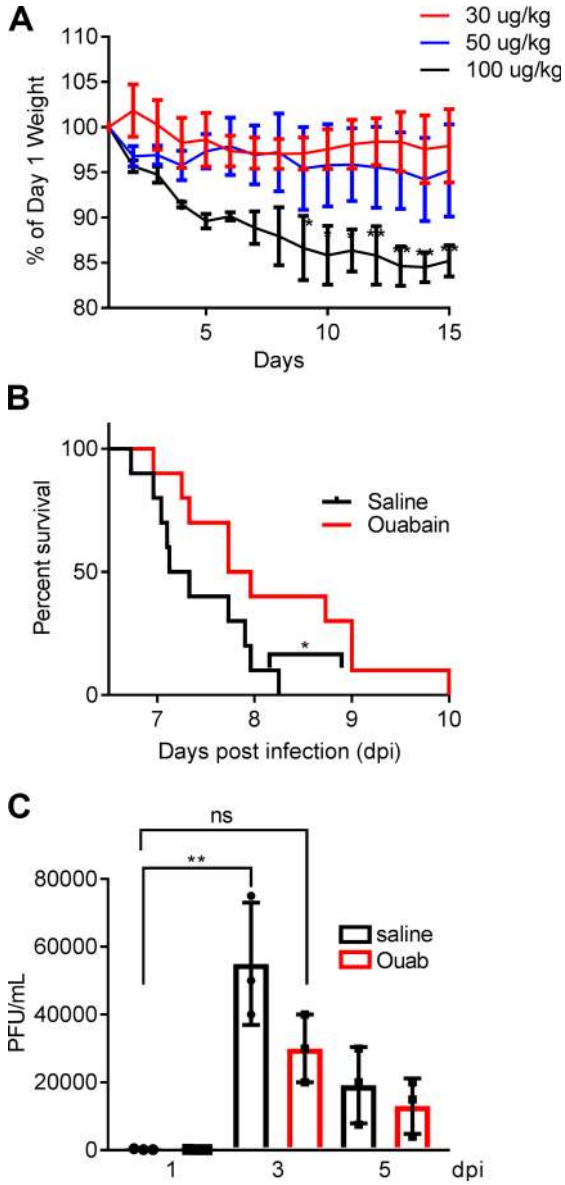

Fig. 6. *A*: cardiac glycoside effects. In vivo $^{S/S}$mice were treated once a day with ouabain at the indicated dose by intraperitoneal injection for 15 consecutive days. Mice were weighed and clinically evaluated daily (n = 3 mice per group). Two-way ANOVA with Sidak's post hoc test. *B*: $^{S/S}$mice were infected with lethal dose of WSN by intratracheal instillation and injected for 2 consecutive days with saline 0.9% NaCl solution or 50 μg/kg body wt of ouabain. Kaplan-Meier mortality curve of mice injected with ouabain is shown (n = 10 mice per group). *$P < 0.05$. *C*: graph represents viral titer [plaque-forming units (PFU)/ml] from lung homogenates harvested from $^{S/S}$mice 1, 3, and 5 days postinfection and treated with saline 0.9% NaCl solution or 50 μg/kg body wt of ouabain (n = 3 mice per group). **$P < 0.01$ and not significant (ns) compared with 1 day postinfection (dpo) determined by one-way ANOVA with Sidak's post hoc test.

(Fig. 6*B*). Moreover, we found that ouabain treatment decreased the IAV viral titers in the lungs of infected mice as compared with saline treated mice (Fig. 6*C*).

DISCUSSION

Influenza virus infection is a highly contagious disease with high prevalence worldwide, causing significant morbidity and mortality (49, 59a). Drug screening studies revealed that CGs are potentially effective against influenza (26). In this study, we uncovered that CGs decrease IAV replication in alveolar epithelial cells and mouse lung tissue via inhibition of cellular protein translation machinery.

We observed that CGs [cardeniolides and bufadenolides (46)] inhibit IAV replication in cell cultures at nanomolar concentrations (Fig. 1, *A–C*) concurring with a previous report in RNA viruses such as Newcastle Disease and Vesicular Stomatitis viruses (26). Our data suggest that ouabain has a strong inhibitory effect even when added after 4 hpi (Fig. 1*I*) and that pretreatment with ouabain does not affect viral replication (Fig. 2*C*), suggesting that CGs interfere with viral translation (3, 23, 28). We found that the influenza A viral proteins NP and M1 were translated between 4 and 6 hpi (Fig. 2*A*) (7) and that ouabain treatment inhibited viral protein abundance (Fig. 2, *E* and *F*). Ouabain is known to affect the cellular proteome (30, 31) and cellular mRNA transcription, decreasing mRNA of cytokines (32) and expression of genes related with differentiation and proliferation (34). We found that although ouabain increased IAV mRNA (Fig. 2*D*), the viral protein abundance was reduced, suggesting that the anti-influenza effect is due to inhibition of viral protein translation. This hypothesis was further supported by data showing that inhibition of the proteasome or lysosomal systems did not prevent the effects of ouabain on the decreased viral protein abundance.

The eukaryotic initiation factor 2 α (eIF2α) is a key factor in the regulation of translation in response to different kinds of cellular stress (including viral infections), and its phosphorylation of Ser51 leads to a decrease in global mRNA translation (19, 48). We found that ouabain induces eIF2α phosphorylation, as previously reported (11), but was not involved in antiviral effects, as IAV replication was still inhibited in mutant cells when the Ser51 of eIF2α was mutated to an alanine (53) (Fig. 3, *B* and *C*). The inhibition of the Na-K-ATPase by ouabain causes significant changes in intracellular ions, increasing Na^+ and decreasing K^+ (30), and can also activate intracellular signaling pathways independently of intracellular cations changes (36). Interestingly, we found that the antiviral effects of the ouabain occurred via the inhibition of the Na-K-ATPase and independently of the Src pathway (Fig. 3*D*).

The intracellular concentration of Na^+ and K^+ cations plays an important role in protein translation (30), as K^+ is necessary for protein biosynthesis (4, 9). We found that ouabain caused a significant decrease in the intracellular K^+ concentration on the same timeline as the antiviral effect, while changes in intracellular Na^+ concentrations happened later (Fig. 3, *G* and *H*). Also, we found that intracellular changes in Ca^{2+} are not related to the anti-influenza effect of CGs (Fig. 3, *I* and *J*), in contrast to the mechanisms described for the inotropic effect of cardiac glycosides on cardiac cells (59).

We found that the inhibition of the Na-K-ATPase and the decrease in intracellular potassium arrested the host cell translation machinery necessary for viral replication (Fig. 4*A*) accordingly to previous reports that have shown similar effects on cytomegalovirus, suggesting a broad effect of this drugs on viral infections (14). Although intracellular K^+ changes can affect intraorganelle pH (10, 57), we showed that initial steps of the influenza cycle are not affected by ouabain (Fig. 2*C*). By

using other means to decrease intracellular potassium, using the ionophore valinomycin or by activating specific voltage- and calcium-dependent potassium channels, we mimicked the effect of ouabain and found similar inhibition of the viral and global protein biosynthesis (Fig. 4, *C–H*).

Short-term treatment with ouabain impaired the viral replication in A549 cells without a significant increase in the cytotoxicity (Fig. 5). We observed a moderate beneficial effect in our in vivo model of IAV infection in $^{S/S}$mice, with a survival improvement when treated with an intraperitoneal injection of ouabain (Fig. 6) compared with saline-injected group. The α-subunit of the Na-K-ATPase is the pharmacological receptor for cardiac glycosides, and rodents have a low-affinity α_1-isoform. We used $^{S/S}$mice, in which the α_1-isoform is rendered ouabain-sensitive via the specific mutations: R111Q and D122N (20). We observed that treating the mice with doses higher than 50 μg/kg of ouabain affected the overall health with significant weight loss as shown in Fig. 6*A*. These data suggest that the levels of ouabain needed to reach a strong inhibition of IAV replication in mice are probably above the toxicity levels, which restricts its systemic use in vivo. The use of CGs at higher doses has the intrinsic limitation that CGs at high doses inhibit alveolar fluid reabsorption, albeit at a dose 10^5 times higher than the one used of the antiviral effect (20 nM ouabain) (51). Higher doses could also be detrimental due to the synergistic effects to the well-known inhibition of Na-K-ATPase in IAV-infected cells (42). Using the dose of 50 μg/kg we showed a moderate improvement in survival in mice treated with ouabain probably due to a decreased viral titer (Fig. 6*C*). Future studies with other delivery options, such as nebulized administration of CGs, or manipulating by other means the intracellular potassium concentration or the translational machinery could provide a novel pharmacological approach to treat influenza infection.

Accordingly, we provide evidence that inhibition of Na-K-ATPase by cardiac glycosides decreases influenza A virus replication by inhibiting the cell protein translational machinery via a decrease in the intracellular potassium. Better understanding of these mechanism should foster the development of more specific therapeutic agents that could be effective and safe to use in patients with influenza virus infection.

ACKNOWLEDGMENTS

We thank Joaquin Hurtado, Melissa Bregger, Ryan Nelson, and Patricia L. Brazee for technical assistance and Marina Casalino-Matsuda, Laura A. Dada, and Karen M. Ridge for support and insightful discussions (Division of Pulmonary and Critical Care Medicine, Northwestern University). Metal analysis was performed at the Northwestern University Quantitative Bioelement Imaging Center generously supported by NASA Ames Research Center NNA06CB93G.

GRANTS

This work was supported in part by National Heart, Lung, and Blood Institute Grant HL-071643.

DISCLAIMERS

The funders had no role in study design, data collection, and interpretation, or the decision to submit the work for publication.

DISCLOSURES

No conflicts of interest, financial or otherwise, are declared by the authors.

AUTHOR CONTRIBUTIONS

L.A., J.K., M.S., L.C.W., H.C., C.P., S.H., E.L., and J.I.S. conceived and designed research; L.A., J.K., M.S., L.C.W., D.C., and E.L. performed experiments; L.A., J.K., M.S., L.C.W., H.C., C.P., S.H., E.L., and J.I.S. analyzed data; L.A., J.K., M.S., L.C.W., C.P., E.L., and J.I.S. interpreted results of experiments; L.A. and E.L. prepared figures; L.A. and E.L. drafted manuscript; E.L. and J.I.S. edited and revised manuscript; J.I.S. approved final version of manuscript.

REFERENCES

1. **Akimova OA, Tverskoi AM, Smolyaninova LV, Mongin AA, Lopina OD, La J, Dulin NO, Orlov SN.** Critical role of the α1-Na^+, K^+-ATPase subunit in insensitivity of rodent cells to cytotoxic action of ouabain. *Apoptosis* 20: 1200–1210, 2015. doi:10.1007/s10495-015-1144-y.
3. **Ashbrook AW, Lentscher AJ, Zamora PF, Silva LA, May NA, Bauer JA, Morrison TE, Dermody TS.** Antagonism of the sodium-potassium ATPase impairs Chikungunya virus infection. *MBio* 7: e00693–e00616, 2016. doi:10.1128/mBio.00693-16.
4. **Austin J, First EA.** Potassium functionally replaces the second lysine of the KMSKS signature sequence in human tyrosyl-tRNA synthetase. *J Biol Chem* 277: 20243–20248, 2002. doi:10.1074/jbc.M201923200.
5. **Aziz Q, Li Y, Anderson N, Ojake L, Tsisanova E, Tinker A.** Molecular and functional characterization of the endothelial ATP-sensitive potassium channel. *J Biol Chem* 292: 17587–17597, 2017. doi:10.1074/jbc.M117.810325.
6. **Bertorello AM, Komarova Y, Smith K, Leibiger IB, Efendiev R, Pedemonte CH, Borisy G, Sznajder JI.** Analysis of Na+,K+-ATPase motion and incorporation into the plasma membrane in response to G protein-coupled receptor signals in living cells. *Mol Biol Cell* 14: 1149–1157, 2003. doi:10.1091/mbc.e02-06-0367.
7. **Boergeling Y, Rozhdestvensky TS, Schmolke M, Resa-Infante P, Robeck T, Randau G, Wolff T, Gabriel G, Brosius J, Ludwig S.** Evidence for a novel mechanism of influenza virus-induced type I interferon expression by a defective RNA-encoded protein. *PLoS Pathog* 11: e1004924, 2015. doi:10.1371/journal.ppat.1004924.
8. **Burkard C, Verheije MH, Haagmans BL, van Kuppeveld FJ, Rottier PJ, Bosch BJ, de Haan CA.** ATP1A1-mediated Src signaling inhibits coronavirus entry into host cells. *J Virol* 89: 4434–4448, 2015. doi:10.1128/JVI.03274-14.
9. **Cahn F, Lubin M.** Inhibition of elongation steps of protein synthesis at reduced potassium concentrations in reticulocytes and reticulocyte lysate. *J Biol Chem* 253: 7798–7803, 1978.
10. **Cang C, Aranda K, Seo YJ, Gasnier B, Ren D.** TMEM175 is an organelle K(+) channel regulating lysosomal function. *Cell* 162: 1101–1112, 2015. doi:10.1016/j.cell.2015.08.002.
11. **Cao J, He L, Lin G, Hu C, Dong R, Zhang J, Zhu H, Hu Y, Wagner CR, He Q, Yang B.** Cap-dependent translation initiation factor, eIF4E, is the target for ouabain-mediated inhibition of HIF-1α. *Biochem Pharmacol* 89: 20–30, 2014. doi:10.1016/j.bcp.2013.12.002.
12. **Chen D, Song M, Mohamad O, Yu SP.** Inhibition of Na+/K+-ATPase induces hybrid cell death and enhanced sensitivity to chemotherapy in human glioblastoma cells. *BMC Cancer* 14: 716, 2014. doi:10.1186/1471-2407-14-716.
13. **Coates BM, Staricha KL, Ravindran N, Koch CM, Cheng Y, Davis JM, Shumaker DK, Ridge KM.** Inhibition of the NOD-like receptor protein 3 inflammasome is protective in juvenile influenza S virus infection. *Front Immunol* 8: 782, 2017. doi:10.3389/fimmu.2017.00782.
14. **Cohen T, Williams JD, Opperman TJ, Sanchez R, Lurain NS, Tortorella D.** Convallatoxin-induced reduction of methionine import effectively inhibits human cytomegalovirus infection and replication. *J Virol* 90: 10715–10727, 2016. doi:10.1128/JVI.01050-16.
15. **Cornelius F, Kanai R, Toyoshima C.** A structural view on the functional importance of the sugar moiety and steroid hydroxyls of cardiotonic steroids in binding to Na,K-ATPase. *J Biol Chem* 288: 6602–6616, 2013. doi:10.1074/jbc.M112.442137.
16. **Crambert G, Hasler U, Beggah AT, Yu C, Modyanov NN, Horisberger JD, Lelièvre L, Geering K.** Transport and pharmacological properties of nine different human Na, K-ATPase isozymes. *J Biol Chem* 275: 1976–1986, 2000. doi:10.1074/jbc.275.3.1976.
17. **Dey M, Cao C, Dar AC, Tamura T, Ozato K, Sicheri F, Dever TE.** Mechanistic link between PKR dimerization, autophosphorylation, and eIF2alpha substrate recognition. *Cell* 122: 901–913, 2005. doi:10.1016/j.cell.2005.06.041.

18. **Dodson AW, Taylor TJ, Knipe DM, Coen DM.** Inhibitors of the sodium potassium ATPase that impair herpes simplex virus replication identified via a chemical screening approach. *Virology* 366: 340–348, 2007. doi:10.1016/j.virol.2007.05.001.
19. **Donnelly N, Gorman AM, Gupta S, Samali A.** The eIF2α kinases: their structures and functions. *Cell Mol Life Sci* 70: 3493–3511, 2013. doi:10.1007/s00018-012-1252-6.
20. **Dostanic I, Schultz JJ, Lorenz JN, Lingrel JB.** The alpha 1 isoform of Na,K-ATPase regulates cardiac contractility and functionally interacts and co-localizes with the Na/Ca exchanger in heart. *J Biol Chem* 279: 54053–54061, 2004. doi:10.1074/jbc.M410737200.
21. **Dowall SD, Bewley K, Watson RJ, Vasan SS, Ghosh C, Konai MM, Gausdal G, Lorens JB, Long J, Barclay W, Garcia-Dorival I, Hiscox J, Bosworth A, Taylor I, Easterbrook L, Pitman J, Summers S, Chan-Pensley J, Funnell S, Vipond J, Charlton S, Haldar J, Hewson R, Carroll MW.** Antiviral screening of multiple compounds against Ebola virus. *Viruses* 8: e277, 2016. doi:10.3390/v8110277.
22. **Duncan R, Hershey JW.** Regulation of initiation factors during translational repression caused by serum depletion. Abundance, synthesis, and turnover rates. *J Biol Chem* 260: 5486–5492, 1985.
23. **Grosso F, Stoilov P, Lingwood C, Brown M, Cochrane A.** Suppression of adenovirus replication by cardiotonic steroids. *J Virol* 91: e01623–e01616, 2017. doi:10.1128/JVI.01623-16.
24. **Haas M, Askari A, Xie Z.** Involvement of Src and epidermal growth factor receptor in the signal-transducing function of Na+/K+-ATPase. *J Biol Chem* 275: 27832–27837, 2000. doi:10.1074/jbc.M002951200.
25. **Hauptman PJ, Kelly RA.** Digitalis. *Circulation* 99: 1265–1270, 1999. doi:10.1161/01.CIR.99.9.1265.
26. **Hoffmann HH, Palese P, Shaw ML.** Modulation of influenza virus replication by alteration of sodium ion transport and protein kinase C activity. *Antiviral Res* 80: 124–134, 2008. doi:10.1016/j.antiviral.2008.05.008.
27. **Jing X, Ma C, Ohigashi Y, Oliveira FA, Jardetzky TS, Pinto LH, Lamb RA.** Functional studies indicate amantadine binds to the pore of the influenza A virus M2 proton-selective ion channel. *Proc Natl Acad Sci USA* 105: 10967–10972, 2008. doi:10.1073/pnas.0804958105.
28. **Kapoor A, Cai H, Forman M, He R, Shamay M, Arav-Boger R.** Human cytomegalovirus inhibition by cardiac glycosides: evidence for involvement of the HERG gene. *Antimicrob Agents Chemother* 56: 4891–4899, 2012. doi:10.1128/AAC.00898-12.
29. **Kirchhof P, Benussi S, Kotecha D, Ahlsson A, Atar D, Casadei B, Castella M, Diener HC, Heidbuchel H, Hendriks J, Hindricks G, Manolis AS, Oldgren J, Popescu BA, Schotten U, Van Putte B, Vardas P, ESC Scientific Document Group.** 2016 ESC Guidelines for the management of atrial fibrillation developed in collaboration with EACTS. *Eur Heart J* 37: 2893–2962, 2016. doi:10.1093/eurheartj/ehw210.
30. **Klimanova EA, Tverskoi AM, Koltsova SV, Sidorenko SV, Lopina OD, Tremblay J, Hamet P, Kapilevich LV, Orlov SN.** Time- and dose dependent actions of cardiotonic steroids on transcriptome and intracellular content of Na^+ and K^+: a comparative analysis. *Sci Rep* 7: 45403, 2017. doi:10.1038/srep45403.
31. **Koltsova SV, Trushina Y, Haloui M, Akimova OA, Tremblay J, Hamet P, Orlov SN.** Ubiquitous [Na+]i/[K+]i-sensitive transcriptome in mammalian cells: evidence for Ca(2+)i-independent excitation-transcription coupling. *PLoS One* 7: e38032, 2012. doi:10.1371/journal.pone.0038032.
32. **La J, Reed E, Chan L, Smolyaninova LV, Akomova OA, Mutlu GM, Orlov SN, Dulin NO.** Downregulation of TGF-β receptor-2 expression and signaling through inhibition of Na/K-ATPase. *PLoS One* 11: e0168363, 2016. doi:10.1371/journal.pone.0168363.
33. **Levenson R, Racaniello V, Albritton L, Housman D.** Molecular cloning of the mouse ouabain-resistance gene. *Proc Natl Acad Sci USA* 81: 1489–1493, 1984. doi:10.1073/pnas.81.5.1489.
34. **Li J, Khodus GR, Kruusmägi M, Kamali-Zare P, Liu XL, Eklöf AC, Zelenin S, Brismar H, Aperia A.** Ouabain protects against adverse developmental programming of the kidney. *Nat Commun* 1: 42, 2010. doi:10.1038/ncomms1043.
35. **Li MM, MacDonald MR, Rice CM.** To translate, or not to translate: viral and host mRNA regulation by interferon-stimulated genes. *Trends Cell Biol* 25: 320–329, 2015. doi:10.1016/j.tcb.2015.02.001.
36. **Liu J, Tian J, Haas M, Shapiro JI, Askari A, Xie Z.** Ouabain interaction with cardiac Na+/K+-ATPase initiates signal cascades independent of changes in intracellular Na+ and Ca2+ concentrations. *J Biol Chem* 275: 27838–27844, 2000.
37. **Luig C, Köther K, Dudek SE, Gaestel M, Hiscott J, Wixler V, Ludwig S.** MAP kinase-activated protein kinases 2 and 3 are required for influenza A virus propagation and act via inhibition of PKR. *FASEB J* 24: 4068–4077, 2010. doi:10.1096/fj.10-158766.
38. **Menger L, Vacchelli E, Adjemian S, Martins I, Ma Y, Shen S, Yamazaki T, Sukkurwala AQ, Michaud M, Mignot G, Schlemmer F, Sulpice E, Locher C, Gidrol X, Ghiringhelli F, Modjtahedi N, Galluzzi L, André F, Zitvogel L, Kepp O, Kroemer G.** Cardiac glycosides exert anticancer effects by inducing immunogenic cell death. *Sci Transl Med* 4: 143ra99, 2012. doi:10.1126/scitranslmed.3003807.
39. **Morales-Nebreda L, Chi M, Lecuona E, Chandel NS, Dada LA, Ridge K, Soberanes S, Nigdelioglu R, Sznajder JI, Mutlu GM, Budinger GR, Radigan KA.** Intratracheal administration of influenza virus is superior to intranasal administration as a model of acute lung injury. *J Virol Methods* 209: 116–120, 2014. doi:10.1016/j.jviromet.2014.09.004.
40. **Nayak DP, Hui EK, Barman S.** Assembly and budding of influenza virus. *Virus Res* 106: 147–165, 2004. doi:10.1016/j.virusres.2004.08.012.
41. **Orlov SN, Thorin-Trescases N, Kotelevtsev SV, Tremblay J, Hamet P.** Inversion of the intracellular Na+/K+ ratio blocks apoptosis in vascular smooth muscle at a site upstream of caspase-3. *J Biol Chem* 274: 16545–16552, 1999. doi:10.1074/jbc.274.23.16545.
42. **Peteranderl C, Morales-Nebreda L, Selvakumar B, Lecuona E, Vadász I, Morty RE, Schmoldt C, Bespalowa J, Wolff T, Pleschka S, Mayer K, Gattenloehner S, Fink L, Lohmeyer J, Seeger W, Sznajder JI, Mutlu GM, Budinger GR, Herold S.** Macrophage-epithelial paracrine crosstalk inhibits lung edema clearance during influenza infection. *J Clin Invest* 126: 1566–1580, 2016. doi:10.1172/JCI83931.
43. **Pinto LH, Holsinger LJ, Lamb RA.** Influenza virus M2 protein has ion channel activity. *Cell* 69: 517–528, 1992. doi:10.1016/0092-8674(92)90452-I.
44. **Pleschka S, Wolff T, Ehrhardt C, Hobom G, Planz O, Rapp UR, Ludwig S.** Influenza virus propagation is impaired by inhibition of the Raf/MEK/ERK signalling cascade. *Nat Cell Biol* 3: 301–305, 2001. doi:10.1038/35060098.
45. **Ponikowski P, Voors AA, Anker SD, Bueno H, Cleland JGF, Coats AJS, Falk V, González-Juanatey JR, Harjola VP, Jankowska EA, Jessup M, Linde C, Nihoyannopoulos P, Parissis JT, Pieske B, Riley JP, Rosano GM, Ruilope LM, Ruschitzka F, Rutten FH, van der Meer P; ESC Scientific Document Group.** 2016 ESC Guidelines for the diagnosis and treatment of acute and chronic heart failure: The Task Force for the diagnosis and treatment of acute and chronic heart failure of the European Society of Cardiology (ESC)Developed with the special contribution of the Heart Failure Association (HFA) of the ESC. *Eur Heart J* 37: 2129–2200, 2016. doi:10.1093/eurheartj/ehw128.
46. **Prassas I, Diamandis EP.** Novel therapeutic applications of cardiac glycosides. *Nat Rev Drug Discov* 7: 926–935, 2008. doi:10.1038/nrd2682.
47. **Reeves JP, Hale CC.** The stoichiometry of the cardiac sodium-calcium exchange system. *J Biol Chem* 259: 7733–7739, 1984.
48. **Rojas M, Arias CF, López S.** Protein kinase R is responsible for the phosphorylation of eIF2alpha in rotavirus infection. *J Virol* 84: 10457–10466, 2010. doi:10.1128/JVI.00625-10.
49. **Rolfes MA, Foppa IM, Garg S, Flannery B, Brammer L, Singleton JA, Burns E, Jernigan D, Reed C, Olsen S, Bresee J.** *Estimated Influenza Illnesses, Medical Visits, Hospitalizations, and Deaths Averted by Vaccination in the United States*. https://www.cdc.gov/flu/about/disease/2015-16.htm. [2016]
50. **Rose L, Jenkins AT.** The effect of the ionophore valinomycin on biomimetic solid supported lipid DPPTE/EPC membranes. *Bioelectrochemistry* 70: 387–393, 2007. doi:10.1016/j.bioelechem.2006.05.009.
51. **Sakuma T, Okaniwa G, Nakada T, Nishimura T, Fujimura S, Matthay MA.** Alveolar fluid clearance in the resected human lung. *Am J Respir Crit Care Med* 150: 305–310, 1994. doi:10.1164/ajrccm.150.2.8049807.
52. **Salata JJ, Jurkiewicz NK, Wang J, Evans BE, Orme HT, Sanguinetti MC.** A novel benzodiazepine that activates cardiac slow delayed rectifier K+ currents. *Mol Pharmacol* 54: 220–230, 1998. doi:10.1124/mol.54.1.220.
53. **Scheuner D, Song B, McEwen E, Liu C, Laybutt R, Gillespie P, Saunders T, Bonner-Weir S, Kaufman RJ.** Translational control is required for the unfolded protein response and in vivo glucose homeostasis. *Mol Cell* 7: 1165–1176, 2001. doi:10.1016/S1097-2765(01)00265-9.
54. **Schmidt EK, Clavarino G, Ceppi M, Pierre P.** SUnSET, a nonradioactive method to monitor protein synthesis. *Nat Methods* 6: 275–277, 2009. doi:10.1038/nmeth.1314.

55. **Siewert E, Müller-Esterl W, Starr R, Heinrich PC, Schaper F.** Different protein turnover of interleukin-6-type cytokine signalling components. *Eur J Biochem* 265: 251–257, 1999. doi:10.1046/j.1432-1327.1999.00719.x.
56. **Sipahi I, Celik S, Tozun N.** A comparison of results of the US food and drug administration's mini-sentinel program with randomized clinical trials: the case of gastrointestinal tract bleeding with dabigatran. *JAMA Intern Med* 174: 150–151, 2014. doi:10.1001/jamainternmed.2013.12217.
57. **Steinberg BE, Huynh KK, Brodovitch A, Jabs S, Stauber T, Jentsch TJ, Grinstein S.** A cation counterflux supports lysosomal acidification. *J Cell Biol* 189: 1171–1186, 2010. doi:10.1083/jcb.200911083.
58. **Weis W, Brown JH, Cusack S, Paulson JC, Skehel JJ, Wiley DC.** Structure of the influenza virus haemagglutinin complexed with its receptor, sialic acid. *Nature* 333: 426–431, 1988. doi:10.1038/333426a0.
59. **Wier WG, Hess P.** Excitation-contraction coupling in cardiac Purkinje fibers. Effects of cardiotonic steroids on the intracellular [Ca2+] transient, membrane potential, and contraction. *J Gen Physiol* 83: 395–415, 1984. doi:10.1085/jgp.83.3.395.
59a. **World Health Organization.** *Influenza (Seasonal): Fact Sheet Nov. 2016* (Online). https://www.who.int/mediacentre/factsheets/fs211/en/. [20 October 2017].